

## NUMERICAL SIMULATION OF CONCRETE BEAMS REINFORCED WITH MIXED RECYCLED/INDUSTRIAL STEEL FIBERS

Enzo Martinelli<sup>a</sup>, Antonio Caggiano<sup>b</sup>, Hernan D. Xargay<sup>b</sup>, Paula C. Folino<sup>b</sup> and  
Guillermo J. Etse<sup>b,c</sup>

<sup>a</sup>*Department of Civil Engineering, Faculty of Engineering, University of Salerno, Fisciano (SA), Italy.  
Email: e.martinelli@unisa.it*

<sup>b</sup>*LMNI, Intecin-CONICET, FIUBA, Materials and Structures Laboratory, Faculty of Engineering,  
University of Buenos Aires, Argentina. Emails: acaggiano@fi.uba.ar, hxargay@fi.uba.ar,  
pfolino@fi.uba.ar*

<sup>b</sup>*CEMNCI, CONICET, Center for Numerical and Computational Methods in Engineering, Faculty for  
Exact Sciences and Technology, National University of Tucuman, Argentina. Email:  
getse@herrera.unt.edu.ar*

**Keywords:** FRC, Waste Tyres, Recycled Fibers, Crack Hinge Model, Fracture Mechanics.

**Abstract.** The disposal of waste tyres represents a big issue in waste management and, then, several recycling procedures have been investigated and in the last decade. One of them consists of partially replacing “natural” constituents of concrete (i.e., aggregates and fibers) with recycled ones derived by waste tyres (e.g., rubber particles in concretes and recycled steel reinforcements), in view of the twofold objective of reducing both the demand of raw materials and the amount of waste to be disposed in landfills. Therefore, a research study is proposed herein to investigate the mechanical behaviour of concrete reinforced with Recycled Steel Fibers (RSFs) recovered from waste tyres. Particularly, the results of an experimental activity carried out on Fiber-Reinforced Concrete (FRC) obtained by mixing Industrial Steel Fibers (ISFs) and RSFs are briefly presented. The structural behaviour of FRC beams in bending has been evaluated in terms of traction-separation law and the possible synergy/replaceability of both fiber types has been investigated. A non-linear cracked hinge model is also presented through an appropriate fracture-based formulation, with the aim of simulating the crack-bridging mechanisms of steel fibers. Then, comparisons between experimental results and numerical predictions are discussed. Both the experimental analysis and the theoretical formulation proposed in this work stem out from the European Project “EnCoRe” (FP7-PEOPLE-2011-IRSES n. 295283; [www.encore-fp7.unisa.it](http://www.encore-fp7.unisa.it)) funded by the European Union as part of the Seventh Framework Programme.

## 1 INTRODUCTION

As it is widely known, concrete is characterised by low tensile (and bending) strength, ductility and energy absorption capacity. Therefore, improving concrete toughness and reducing the size and amount of defects in concrete would lead to enhance its resulting mechanical performance. As a matter of fact, adding a small fraction (usually in the order of 0.5 – 1.0% in volume) of short fibers during mixing is an effective way to improve the toughness of concrete and obtain a material which is generally referred to as Fiber-Reinforced Cementitious Composite (FRCC) and can be further classified in Fiber-Reinforced Concrete (FRC) or Fiber-Reinforced Mortar (FRM), depending on the aggregate sizes within the cementitious matrix. In the fracture process of FRCC materials, fibers bridging active cracks can provide resistance to crack propagation and crack opening before being either pulled out or stressed to rupture (Naaman and Reinhardt, 2006).

Fibers for FRCC generally need to be durable within the cementitious environment, be easy to spread in concrete mix, have good mechanical properties and be of appropriate geometric configuration in order to be effective (Qian et al., 2003). Many fibers have been used for concrete reinforcement and some are widely available for commercial applications. They include steel, glass, natural cellulose, carbon, nylon, polypropylene, etc. (ACI-544.1-96, 1996). Since the annual world fiber market amounts to about 60 million tonnes, including natural and man-made fibers, the increased ecological awareness and the more severe legislation for waste disposal led to an increased interest towards the possible production of structural fibers via recycling processes (Bartl et al., 2005).

Plenty of rubber tyres are replaced every year and need to be disposed, with huge implications on the environment. There is a strong motivation for implementing and realising recycling processes of such waste materials which can be easily turned into a wealthy source for producing secondary raw materials. In this framework, steel fibers can be derived by disassembling the internal metallic structure of exhausted tyres and, then, employed as a dispersed reinforcement in cement-based composites (Yung et al., 2013). Moreover, rubber scraps can also be employed in partial replacement of concrete aggregates (Centonze et al., 2012).

Innovative researches on FRC also address the possible use of mixed fibers of different material and/or geometry which can, in principle, play a synergistic role in enhancing flexural and post-cracking response of structural members. This kind of fiber-reinforced cement-based composites are often referred to as Hybrid FRC (HyFRC). Experimental tests aimed at investigating the HyFRC failure behaviour in direct tension have been performed, among others, by Sorelli et al. (2005) and Park et al. (2012). The mechanical behaviour measured by means of indirect tensile tests have been proposed on Hy-Polypropylene FRC (Hsie et al., 2008), Hy-Steel FRC (Kim et al., 2011) or combining several material fibers: i.e., Carbon/Steel/Polypropylene FRC (Yao et al., 2003) or Steel/Palm/Synthetic FRC (Dawood and Ramli, 2012). Other relevant contributions regarding HyFRC with lightweight aggregates (Libre et al., 2011), high-volume coarse fly ash (Sahmaran and Yaman, 2007), HyFRC exposed to high temperatures (Ding et al., 2012) or self compacting HyFRC (Akçay and Tasdemir, 2012) have also been proposed within the scientific community.

From the modelling point of view, it has become widely accepted that the post-cracking behaviour of FRC may be effectively described through the concepts of “fictitious crack model”. This simple formulation was originally developed for plain concrete by Hillerborg et al. (1976) and later extended to FRC in several works, a.o., Olesen (2001), Park et al. (2010) and Buratti et al. (2011).

This paper briefly summarises the results of an experimental campaign carried out on Fiber-Reinforced Concrete (FRC) obtained by mixing industrial (hooked-end) and recycled (deriving from waste tyres) steel fibers. The experimental campaign was aimed at observing the key aspects of the mechanical behaviour of Hybrid Industrial/Recycled Steel Fiber-Reinforced Concrete (HIRSFRC) in bending. The structural behaviour was evaluated in terms of tension-separation law for FRC and was intended to unveil the possible synergistic effect of combining the two kinds of aforementioned fibers. Such a campaign is assumed as a benchmark for the numerical simulations proposed in this work.

A simple model is presented in this paper to take into account the fiber-matrix interactions, though within the framework of a “cracked-hinge” approach, which appears as a more feasible method to perform “structural scale” simulations of FRCC members loaded in bending. The model represents a straightforward extension of the proposal presented by Olesen (2001). The bridging mechanisms of fibers in FRCC is introduced by means of the explicit modelling proposed by the authors in Caggiano et al. (2012a) to obtain a meso-mechanical interpolation of the complex interactions actually developing between fibers and matrix.

After this introduction, Section 2 describes the analysed FRC mixes. Then, Section 3 highlights the formulation of the proposed crack-hinge model for simulating the observed cracking and post-cracking behaviour of HIRSFRC specimens. Comparisons between experimental data and numerical predictions are presented and discussed in Section 4, then, Section 5 remarks the key results of the present research and figures out its possible future steps.

## 2 EXPERIMENTAL CAMPAIGN

Several specimens were fabricated and tested for examining the mechanical properties of plain and fiber-reinforced concrete. Four mixes, made with two different types of steel fibers, were considered. Moreover, a mix of plain concrete without fibers was taken as a reference (labelled as “REF”). The tests were performed according to UNI-11039-1 (2003) and UNI-11039-2 (2003) standards.

### 2.1 Industrial and recycled steel fibers

Two types of steel reinforcements were employed in FRCs: (i) Wirand Fibers FS7 type (“Industrial”) as shown in Figure 1 and (ii) steel fibers recovered from waste tyres (“Recycled”) as shown in Figure 2.



Figure 1: Wirand Fibers FS7 industrial steel fiber.

The following geometric and mechanical properties characterise such fibers employed in this research:



Figure 2: Recycled steel fibers: (a) previous the selection of the coarse pieces, (b) separating the coarse reinforcements and (c) the employed fibers.

- industrial steel fibers:  $l_f = 33 \text{ mm}$  (length);  $d_f = 0.55 \text{ mm}$  (diameter),  $AR = 60$  (aspect ratio) and  $f_t > 1200 \text{ MPa}$  (failure strength);
- recycled steel fibers:  $l_{f,m} = 12 \text{ mm}$  (average value of the lengths);  $d_{f,m} = 0.27 \text{ mm}$  (average value of the diameters),  $AR_m = 44$  (average value of the aspect ratios) and  $f_{t,m} > 1200 \text{ MPa}$  (main failure strength).

The complete geometric studies and the mechanical characterisation of the RSFs is reported in the [D1.3-Encore-Report \(2013\)](#).

## 2.2 Test programme

Experimental tests were carried out according to the procedures described in [UNI-11039-1 \(2003\)](#) and [UNI-11039-2 \(2003\)](#). Particularly, prismatic  $150 \times 150 \times 600 \text{ mm}^3$  specimens were tested under four-point bending as shown in [Figure 3](#).

Each specimen was preliminarily notched (through a  $2.0 \text{ mm}$  wide-slit) of  $45 \text{ mm}$  depth and starting from the bottom surface of the sample. The specimens were tested under displacement control (having displacement rate of  $0.005 \text{ mm/sec}$ ) and recording load by means of a load-cell, displacements and crack openings. The latter were measured by means of dedicated displacement transducers which monitored the relative displacements of the two sides of the notch.

Two series of specimens were tested:

- plain or reference (REF) concrete specimens;



Figure 3: Four-point beam test according to [UNI-11039-2 \(2003\)](#).

- steel fiber-reinforced specimens with 0.5 % of fiber content.

The complete experimental programme is highlighted in Table 1. The first column of the table reports a label denoting the mixture and provides key information about the type and content of fibers. Particularly, after the RSFRC (Recycled Steel Fiber Reinforced Concrete) label, the first number indicates the type of industrial-to-recycled substitution while the second one reports the fiber volume fraction. As example, *RSFRC25 – 05* represents a HIRSFRC characterised by the 25% of recycled fibers while the remaining 75% of industrial ones. The second code also indicates a 0.5% of fiber volume fraction of such mix. For each mix, three beams were cast and tested under four-point bending. Moreover, three cubes of  $150 \times 150 \times 150 \text{ mm}^3$  were also cast and tested for measuring the compressive strength developed by the SFRC mixes.

Table 1: Experimental programme.

| Mixtures            | Compression tests (28 days) | Four-Point Bending Beams (28 days) |
|---------------------|-----------------------------|------------------------------------|
| "REF"               | 3                           | 3                                  |
| <i>RSFRC 0-05</i>   | 3                           | 3                                  |
| <i>RSFRC 25-05</i>  | 3                           | 3                                  |
| <i>RSFRC 50-05</i>  | 3                           | 3                                  |
| <i>RSFRC 100-05</i> | 3                           | 3                                  |

A thorough and detailed description of the experimental results can be found in the [D1.3-Encore-Report \(2013\)](#) and is herein omitted for the sake of brevity.

### 3 CRACKED HINGE NUMERICAL MODEL FOR FIBER-REINFORCED CONCRETE

The model formulation outlined in this section is based on the original proposal by [Olesen \(2001\)](#) where a non-linear cracked hinge model was developed with the aim to analyse the bending fracture behaviour of fiber-reinforced concrete beams. Similar proposals for simulating the fracture behaviour of both plain and SFRC members have been proposed in literature a.o. by [Zhang and Li \(2004\)](#), [Oh et al. \(2007\)](#) and [Walter and Olesen \(2008\)](#).

According to the fictitious crack method ([Olesen, 2001](#)), the following stress-strain and stress-crack opening relationships can be written in the notched section of Figure 4

$$\sigma_{SFRC} = E \cdot \varepsilon \quad (1)$$

$$\sigma_{SFRC} = \sigma [u_{cr}] + \sum_{f=0}^{n_f} [\sigma_f [u_{N,cr}] n_{N,f} + \tau_f [u_{T,cr}] n_{T,f}] \quad (2)$$

being  $\sigma_{SFRC}$  the stress of the considered cementitious composite,  $E$  the concrete elastic modulus,  $\varepsilon$  the elastic strain and  $\sigma [u_{cr}]$  the stress-crack opening law of the plain concrete;  $\sigma_f$  and  $\tau_f$  mean the bond-slip and dowel actions of the single considered reinforcement which are related to axial and tangential cracking displacements,  $u_{N,cr}$  and  $u_{T,cr}$  at fiber level, respectively (Figure 5). Moreover,  $n_{N,f}$  and  $n_{T,f}$  are the direction cosines of the fiber for its normal and tangential direction, respectively. Finally,  $n_f$  represents the number of fibers crossing the analysed strip in the crack section, considering, for simplicity, that each generic fiber crosses the fracture line at its mid-length,  $l_{emb} = l_f/2$ .

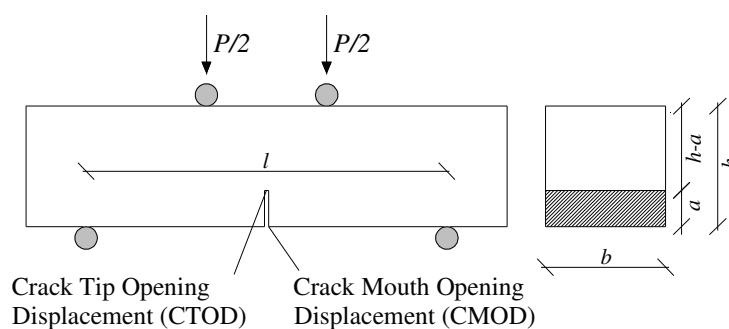


Figure 4: Geometrical description of the analysed four-point bending scheme.

As a matter of principle, Eq. (2) is the same one proposed in [Caggiano et al. \(2012a\)](#) and also employed in more general meso-scale models in [Etse et al. \(2012\)](#).

The considered direction cosines for each fiber, given in Eq. (2), are finally defined as follows

$$n_{N,f} = \cos \vartheta \cos \varpi; \quad n_{T,f} = \sin \vartheta \cos \varpi \quad (3)$$

being  $\vartheta$  and  $\varpi$  the polar and the azimuthal angles of the single fiber crossing the crack surface.

The number of crossing fibers per strip,  $n_f$ , is evaluated through the formula proposed by [Dupont and Vandewalle \(2005\)](#)

$$n_f = \alpha_N \frac{\rho_f}{A_f} A_i \quad (4)$$

where  $\rho_f$  is the fiber content,  $A_f$  and  $A_i$  the cross-sectional areas of a single fiber and the interface ( $A_i = b \cdot h_s$ , being  $b$  the base width and  $h_s$  the height of the analysed strip), respectively.

The orientation factor can be estimated by means of the following relationship (Dupont and Vandewalle, 2005)

$$\alpha_{\bar{N}} = \frac{\alpha_{\bar{N},1} \cdot (b - l_f)(h - l_f) + \alpha_{\bar{N},2} \cdot [(b - l_f)l_f + (h - l_f)l_f] + \alpha_{\bar{N},3} \cdot l_f^2}{b \cdot h} \quad (5)$$

by geometrically averaging the orientation factors  $\alpha_{\bar{N},1}$ ,  $\alpha_{\bar{N},2}$  and  $\alpha_{\bar{N},3}$ , referred to the zone 1, 2 and 3 of the square cross section beam (Figure 6).

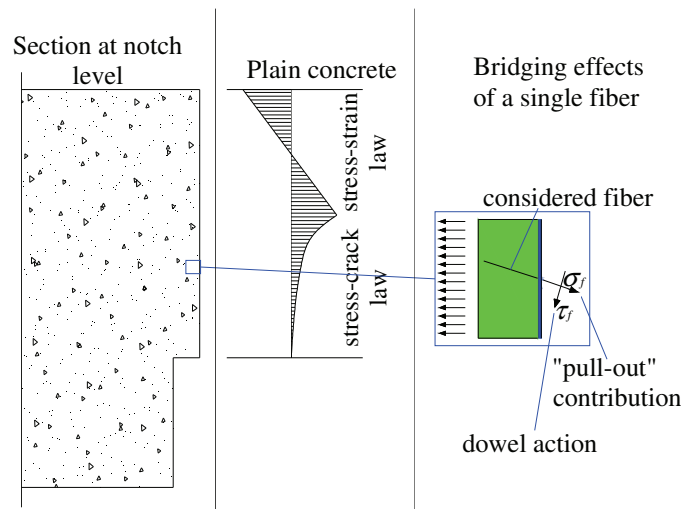


Figure 5: Stress distributions and fiber actions during the crack evolution.

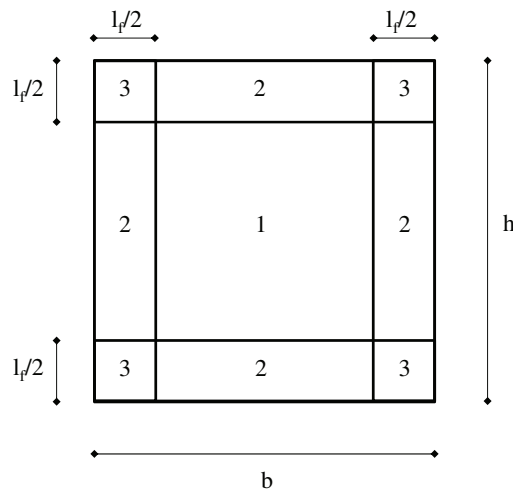


Figure 6: The three orientation zones for the square cross section beam:  $b \times h \times l$  (base  $\times$  height  $\times$  length) having  $l \geq b$  and  $l \geq h$ .

The stress-crack opening relationship,  $\sigma [u_{cr}]$ , of plain concrete matrix is based on the interface law proposed by Carol et al. (1997) and considering the case of pure tension. Particularly,

the interface loading criterion, the flow rule and the softening (evolution) law are defined as

$$\begin{aligned} f(\sigma, \kappa) &= \sigma^2 - \sigma_y^2 \leq 0 && \text{loading criterion} \\ \dot{u}_{cr} &= \dot{\lambda} \frac{\partial f}{\partial \sigma} = 2 \cdot \dot{\lambda} \cdot \sigma && \text{plastic flow} \\ \sigma_y &= f_t \left(1 - \frac{w_{cr}}{G_f^I}\right) && \text{evolution law} \end{aligned} \quad (6)$$

where  $\sigma_y$  is the current tensile strength and  $\kappa$  the internal state variable. The incremental cracking displacement,  $\dot{u}_{cr}$ , is defined by means of the classical flow rule, being  $\dot{\lambda}$  the rate of the non-negative plastic multiplier. The variation of  $\sigma_y$  is assumed to be linear, from its maximum value  $f_t$  (tensile strength) to zero, based on the ratio between the work spent and the available fracture energy,  $\frac{w_{cr}}{G_f^I}$ . The rate of fracture work,  $\dot{w}_{cr}$ , is defined as follows

$$\dot{w}_{cr} = \sigma \cdot \dot{u}_{cr}. \quad (7)$$

Based on these hypotheses, the employed model exhibits the following closed-form solution under the well-known Kuhn-Tucker and consistency conditions (Carol et al., 1997; Stankowski et al., 1993)

$$\sigma = f_t \exp\left(-\frac{u_{cr} f_t}{G_f^I}\right) \quad (8)$$

which represents an exponential expression of the  $\sigma - u_{cr}$  law (Figure 7a).

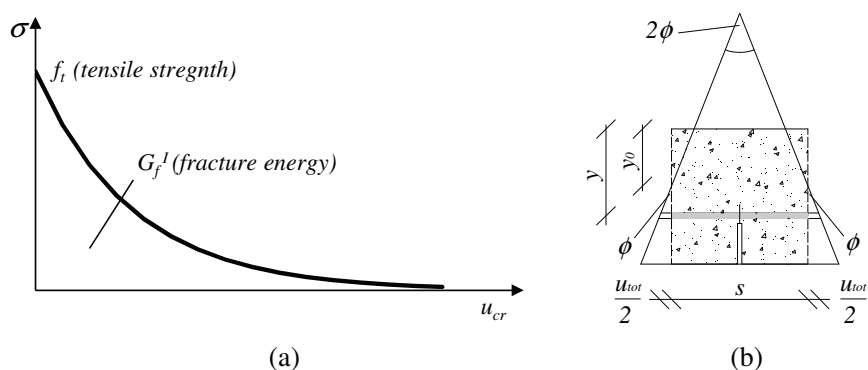


Figure 7: Cracked hinge: (a) stress-crack opening displacement of plain concrete and (b) main geometrical assumption under deformation.

The total crack opening,  $u_{cr}$ , at the considered strip is obtained by subtracting the elastic part from the total displacement  $u_{tot}$ ,

$$u_{cr} = u_{tot} - s \frac{\sigma_{SFRC}[u_{cr}]}{E} \quad (9)$$

where

$$u_{tot} = 2 \cdot \phi \cdot (y - y_0) \quad (10)$$

being  $\phi$  the angular deformation (relative angle of the two end sections of the crack hinge), while  $y$  and  $y_0$  deal with the considered strip position and the depth of the neutral axis as depicted in Figure 7b. In Eq. (9),  $s$  represents the hinge length.

Solving Eq. (9) for  $\sigma_{SFRC}$  and substituting  $u_{tot} = s \cdot \epsilon^*$ , where  $\epsilon^*$  is the mean longitudinal strain in the considered section

$$\epsilon^* = \frac{2 \cdot \phi \cdot (y - y_0)}{s} \tag{11}$$

the following expression for  $\sigma_{SFRC}$  can be obtained

$$\sigma_{SFRC} = \frac{E \cdot 2 \cdot \phi \cdot (y - y_0) - u_{cr}[y]}{s} \tag{12}$$

Now, the expression of  $u_{cr}$ , at the  $y$  level of the considered strip can be obtained by introducing Eqs. (2) and (8) into Eq. (12)

$$u_{cr}[y] = \frac{G_f^I \cdot W \left[ -\frac{f_t^2 \cdot s \cdot \exp\left(-\frac{2 \cdot f_t \cdot \phi \cdot (y - y_0)}{G_f^I} + \frac{s \cdot (\sigma_f + \tau_f)}{E \cdot G_f^I}\right)}{E \cdot G_f^I} \right]}{f_t} + 2 \cdot \phi \cdot (y - y_0) + \frac{s \cdot (\sigma_f + \tau_f)}{E \cdot f_t} \tag{13}$$

where  $W[\dots]$  represents the well-known Lambert W function (also known as product logarithm).

Finally, by adopting the above Eq. (13) into Eq. (8), the following composite stress,  $\sigma_{SFRC}$ , can be obtained

$$\sigma_{SFRC} = f_t \cdot \exp \left( W \left[ -\frac{f_t^2 \cdot s \cdot \exp\left(-\frac{2 \cdot f_t \cdot \phi \cdot (y - y_0)}{G_f^I} + \frac{s \cdot (\sigma_f + \tau_f)}{E \cdot G_f^I}\right)}{E \cdot G_f^I} \right] \right) + (\sigma_f + \tau_f). \tag{14}$$

Once the complete stress distribution is obtained in both elastic and post-cracking states, the external force  $P$  and/or the corresponding bending moment  $M$  can be easily obtained by equilibrium conditions between internal and external forces. Particularly, the equilibrium equation along the axial direction is commonly employed to determine the position of the neutral axis  $y_0$ . Then, the resulting bending moment can be evaluated by means of the rotation equilibrium equation.

Finally, both Crack-Tip and Mouth Opening Displacements ( $CTOD$  and  $CMOD$  as highlighted in Figure 4) can be easily calculated by evaluating  $u_{tot}$  of Eq. (10) for  $y = h - a$  and  $y = h$ , respectively,

$$\begin{aligned} CTOD &= u_{tot}[h - a] \\ CMOD &= u_{tot}[h]. \end{aligned} \tag{15}$$

### 3.1 Bond-slip bridging of fibers on concrete cracks

Fracture opening processes in concrete activate bridging effects induced by fibers. The axial (tensile) stresses in fibers are balanced by bond developing on their lateral surface embedded in concrete matrix. Thus, a simple equilibrium equation can be written

$$\frac{d\sigma_f[x]}{dx} = -\frac{4\tau_a[x]}{d_f} \tag{16}$$

where  $\sigma_f$  is the axial tensile stress developed in fibers and considered in Eq. (2),  $\tau_a$  the local bond stress between fiber and matrix, and  $d_f$  the fiber diameter.

A simplified bilinear bond-slip law is proposed to model the fiber-to-concrete debonding process as follows

$$\tau_a[x] = \begin{cases} -k_E s[x] & s[x] \leq s_e \\ -\tau_{y,a} + k_S (s[x] - s_e) & s_e < s[x] \leq s_u \\ 0 & s[x] > s_u \end{cases} \quad (17)$$

where  $s[x]$  defines the debonded displacement between fiber and concrete (at the point of the abscissa  $x$ ). The positive constants  $k_E$  and  $k_S$  represent the elastic and softening slopes of such bond-slip relationships, respectively;  $\tau_{y,a}$  is the shear bond strength, while  $s_e$  and  $s_u$  are the elastic and ultimate slips, respectively.

This approach is strictly true in the case of considering synthetic fibers, while can be extended for steel ones when the length  $l_{emb}$  results in the condition that  $|\sigma_{f,max}| \leq \sigma_{y,s}$ , where  $\sigma_{f,max}$  and  $\sigma_{y,s}$  represent the maximum axial stress and the steel yielding, respectively. The complete formulation of this numerical model and its validation against bond-slip experimental tests was proposed in a previous work published by the authors in [Caggiano et al. \(2012b\)](#); [Caggiano and Martinelli \(2012\)](#).

### 3.2 Dowel action of fibers crossing the concrete cracks

The dowel mechanism, resulting in a shear transfer action across cracks, represents an important component on the overall interaction between steel fibers and concrete matrix. A simple numerical sub-model for the dowel action is based on defining both stiffness and strength of the generic fiber embedded in the concrete matrix and subjected to a transverse force/displacement at the fracture level. On the one hand, the well-known Winkler beam theory is used to describe the dowel force-displacement relationship, which is transformed in terms of dowel stress vs. relative displacements suitable for the cracked hinge model (namely  $\tau_f [u_{T,cr}]$  of Eq. 2). On the other hand, the empirical model reported by [Dulacska \(1972\)](#) for RC-structures is taken as maximum dowel strength. A thorough and detailed description of the dowel formulation can be found in [Caggiano et al. \(2012a\)](#) and is omitted herein for the sake of brevity.

## 4 COMPARISON BETWEEN EXPERIMENTAL DATA AND NUMERICAL SIMULATIONS

The model outlined in the previous sections is introduced in the cracked hinge zone model with the aim of simulating the behaviour observed for the  $150 \times 150 \times 600 \text{ mm}^3$  notched concrete specimens tested under four-point bending.

To this end, two material types are considered:

- SFRC having  $\rho_f = 0.5\%$  of industrial reinforcements and
- SFRC with  $\rho_f = 0.5\%$  of recycled ones.

The geometric and mechanical properties are chosen according to the tests outlined in the experimental campaign described in Section 2.

The local bond-slip law is determined through an inverse identification on the test results obtained on specimens reinforced with only industrial or recycled fibers with  $\rho_f = 0.5\%$ . Then, the calibrated parameters are used to simulate the behaviour observed in all hybrid tests. Particularly, the mechanical parameters employed in the numerical evaluations are:

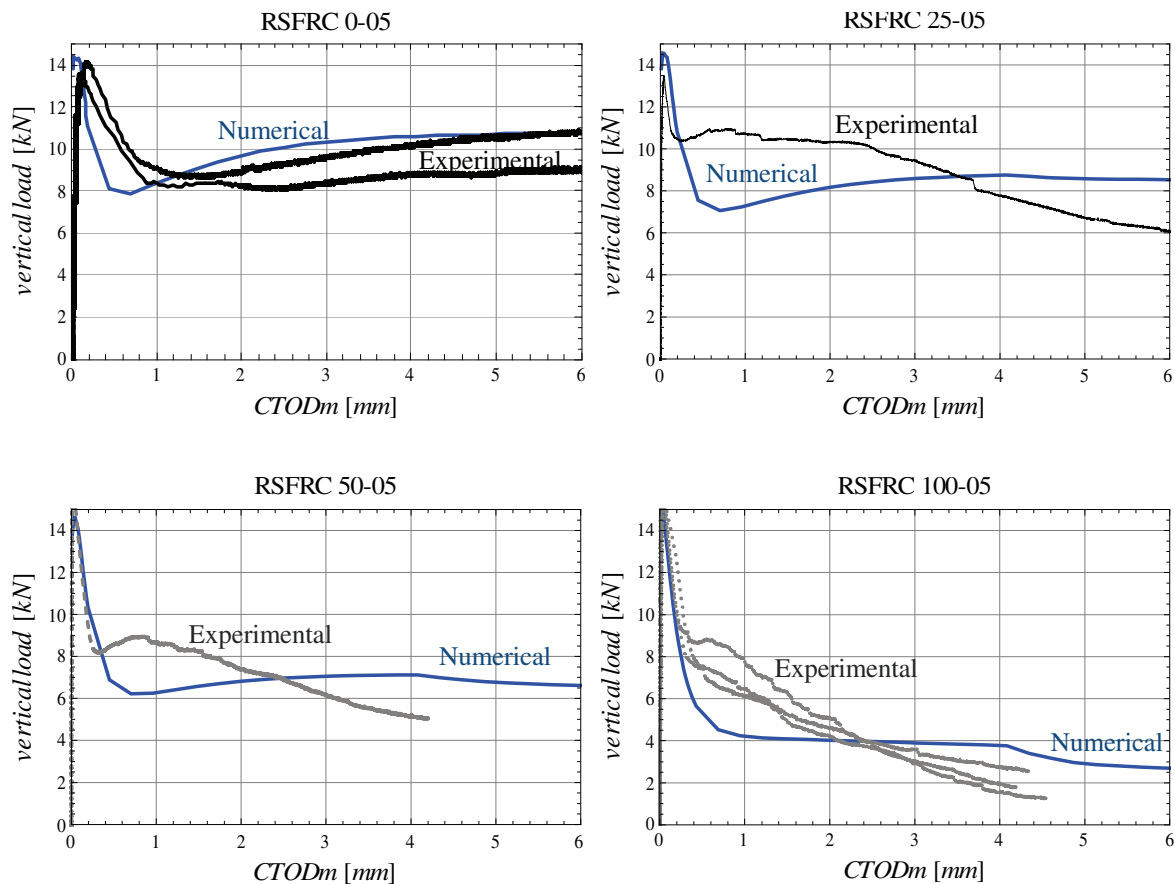


Figure 8: Load- $CTOD_m$  numerical predictions against the experimental data by the [D1.3-Encore-Report \(2013\)](#).

- plain concrete parameters:  $f_t = 2.78$  MPa (tensile strength),  $E = 31.5$  GPa (elastic modulus),  $s = 75$  mm (hinge length),  $G_f^I = 0.5$  N/mm (fracture energy);
- industrial steel fibers:  $\tau_{y,a} = 4.5$  MPa (shear bond strength),  $k_E = 100.0$  N/mm<sup>3</sup> (elastic stiffness),  $k_S = 0.1$  N/mm<sup>3</sup> (softening stiffness),  $k_{dow} = 2.8$  (dowel parameter) and  $c_1 = 0.15$  (coefficient of beam foundation);
- recycled steel fibers:  $\tau_{y,a} = 2.5$  MPa (shear bond strength),  $k_E = 100.0$  N/mm<sup>3</sup> (elastic stiffness),  $k_S = 0.2$  N/mm<sup>3</sup> (softening stiffness),  $k_{dow} = 1.05$  (dowel parameter) and  $c_1 = 0.15$  (coefficient of beam foundation).

The assumed values for the orientation factors  $\alpha_{\bar{N}}$  are based on the theoretical proposal outlined by [Dupont and Vandewalle \(2005\)](#). Particularly, the values 0.5425 and 0.5143 are determined for industrial and steel fibers, respectively.

The numerical force- $CTOD_m$  curves are proposed in Figure 8 along with the corresponding experimental results.  $CTOD_m$  represents the mean of the two opposite Crack Tip Opening Displacements ( $CTOD_s$ ) registered by the transducer devices of the experimental campaign. The load-crack opening responses of HIRSFRC beams emphasize the significant influence of the fiber reinforcement on the strength and the post-cracking behaviour. Fiber bridging effects on the pre-cracked concretes are well simulated by the considered numerical approach with the proposed non-linear separation law for SFRC.

The results of these numerical analyses demonstrate that the model leads to accurate simulations of the HIRSFRC performance in terms of both peak strength and post-peak ductility of failure processes under mode I type of fracture. As a matter of results, the model is able to efficiently reproduce (in explicit way) the combining bridging mechanisms of both recycled and industrial steel fibers.

## 5 CONCLUDING REMARKS

The four-point bending behaviour of notched beams reinforced with mixed recycled/industrial steel fibers was observed in a series of experimental tests outlined at the beginning of this paper. Particularly, four different combinations of industrial/recycled steel were considered in the proposed experiments. Some of this results were considered to calibrate a stress-crack opening model, based on a hinge-crack approach, which was, then, employed to simulate the remaining results obtained in the aforementioned experimental campaign. The numerical predictions, compared with the experimental measures, demonstrate the soundness and capability of the model to reproduce the mechanical response of Hybrid Industrial/Recycled Steel Fiber-Reinforced Concrete (HIRSFRC) components. Further studies are needed for achieving a possibly stable relationship between the amounts of fibers, their typology and the relevant parameters which identify the presented model. These studies are part of future developments of this research.

## ACKNOWLEDGMENT

The authors acknowledge the financial support for this work by CONICET (Argentinian National Council for Science and Technology) through the Grant PIP 112-200801-00707, CIUNT (Research council of the National University of Tucuman) through the Grant 26/E479 and the European Union within the Seventh Framework Programme through the Grant EnCoRe (FP7-PEOPLE-2011-IRSES, n. 295283).

## REFERENCES

- ACI-544.1-96. *State-of-the-Art Report on Fiber Reinforced Concrete. Reported by ACI Committee 544, American Concrete Institute*. 1996.
- Akçay B. and Tasdemir M. Mechanical behaviour and fibre dispersion of hybrid steel fibre reinforced self-compacting concrete. *Construction and Building Materials*, 28(1):287 – 293, 2012.
- Bartl A., Hackl A., Mihalyi B., Wistuba M., and Marini I. Recycling of fibre materials. *Process Safety and Environmental Protection*, 83(B4):351 – 358, 2005.
- Buratti N., Mazzotti C., and Savoia M. Post-cracking behaviour of steel and macro-synthetic fibre-reinforced concretes. *Construction and Building Materials*, 25(5):2713 – 2722, 2011.
- Caggiano A., Etse G., and Martinelli E. Zero-thickness interface model formulation for failure behavior of fiber-reinforced cementitious composites. *Computers & Structures*, 98-99(0):23 – 32, 2012a.
- Caggiano A. and Martinelli E. A unified formulation for simulating the bond behaviour of fibres in cementitious materials. *Materials & Design*, 42(0):204 – 213, 2012.
- Caggiano A., Martinelli E., and Faella C. A fully-analytical approach for modelling the response of FRP plates bonded to a brittle substrate. *Int. J. of Solids and Structures*, 49(17):2291 – 2300, 2012b.
- Carol I., Prat P., and Lopez C. Normal/shear cracking model: Applications to discrete crack

- analysis. *J. of Engrg. Mechanics - ASCE*, 123:765–773, 1997.
- Centonze G., Leone M., and Aiello M. Steel fibers from waste tires as reinforcement in concrete: A mechanical characterization. *Construction and Building Materials*, 36(0):46 – 57, 2012.
- D1.3-Encore-Report. *Experimental Tests on concrete specimens with recycled fibers (UMinho)*. Internal Report of the Project "Environmentally-friendly solutions for Concrete with Recycled and natural components - Grant Agreement Number: PIRSES-GA-2011-295283, 2013.
- Dawood E. and Ramli M. Mechanical properties of high strength flowing concrete with hybrid fibers. *Construction and Building Materials*, 28(1):193 – 200, 2012.
- Ding Y., Azevedo C., Aguiar J., and Jalali S. Study on residual behaviour and flexural toughness of fibre cocktail reinforced self compacting high performance concrete after exposure to high temperature. *Construction and Building Materials*, 26(1):21 – 31, 2012.
- Dulacska H. Dowel action of reinforcement crossing cracks in concrete. *ACI Structural J.*, 69(12):754–757, 1972.
- Dupont D. and Vandewalle L. Distribution of steel fibres in rectangular sections. *Cement and Concrete Composites*, 27(3):391 – 398, 2005.
- Etse G., Caggiano A., and Vrech S. Multiscale failure analysis of fiber reinforced concrete based on a discrete crack model. *International Journal of Fracture*, 178(1-2):131–146, 2012.
- Hillerborg A., Modeer M., and Petersson P. Analysis of crack formation and crack growth in concrete by means of fracture mechanics and finite elements. *Cement and Concrete Composites*, 6(6):773–781, 1976.
- Hsie M., Tu C., and Song P. Mechanical properties of polypropylene hybrid fiber-reinforced concrete. *Materials Science and Engrg.: A*, 494(1 - 2):153 – 157, 2008.
- Kim D., Park S., Ryu G., and Koh K. Comparative flexural behavior of hybrid ultra high performance fiber reinforced concrete with different macro fibers. *Construction and Building Materials*, 25(11):4144 – 4155, 2011.
- Libre N., Shekarchi M., Mahoutian M., and Soroushian P. Mechanical properties of hybrid fiber reinforced lightweight aggregate concrete made with natural pumice. *Construction and Building Materials*, 25(5):2458 – 2464, 2011.
- Naaman A. and Reinhardt H. Proposed classification of HPFRC composites based on their tensile response. *Materials and Structures*, 39:547–555, 2006.
- Oh B., Kim J., and Choi Y. Fracture behavior of concrete members reinforced with structural synthetic fibers. *J. of Engrg. Mechanics - ASCE*, 74:243–257, 2007.
- Olesen J. Fictitious crack propagation in fiber-reinforced concrete beams. *J. of Engrg. Mechanics - ASCE*, 127(3):272–280, 2001.
- Park K., Paulino G., and Roesler J. Cohesive fracture model for functionally graded fiber reinforced concrete. *Cement and Concrete Composites*, 40:956–965, 2010.
- Park S., Kim D., Ryu G., and Koh K. Tensile behavior of ultra high performance hybrid fiber reinforced concrete. *Cement and Concrete Composites*, 34(2):172 – 184, 2012.
- Qian X., Zhou X., Mu B., and Li Z. Fiber alignment and property direction dependency of FRC extrudate. *Cement and Concrete Research*, 33(10):1575 – 1581, 2003.
- Sahmaran M. and Yaman I. Hybrid fiber reinforced self-compacting concrete with a high-volume coarse fly ash. *Construction and Building Materials*, 21(1):150 – 156, 2007.
- Sorelli L., Meda A., and Plizzari G. Bending and uni-axial tensile tests on concrete reinforced with hybrid steel fibers. *ASCE - J. of Materials in Civil Engrg.*, 17(5):519 – 527, 2005.
- Stankowski T., Runesson K., and Sture S. Fracture and slip of interfaces in cementitious composites. I: Characteristics, II: Implementation. *ASCE - J. Engrg. Mech.*, 119(2):292–327, 1993.

- UNI-11039-1. *Steel fibre reinforced concrete - Definitions, classification and designation*. UNI Editions, Milan, Italy, 2003.
- UNI-11039-2. *Steel fibre reinforced concrete - Test method to determine the first crack strength and ductility indexes*. UNI Editions, Milan, Italy, 2003.
- Walter R. and Olesen J.F. Cohesive mixed mode fracture modelling and experiments. *Engrg. Fracture Mechanics*, 75(18):5163 – 5176, 2008.
- Yao W., Li J., and Wu K. Mechanical properties of hybrid fiber-reinforced concrete at low fiber volume fraction. *Cement and Concrete Research*, 33(1):27 – 30, 2003.
- Yung W.H., Yung L.C., and Hua L.H. A study of the durability properties of waste tire rubber applied to self-compacting concrete. *Construction and Building Materials*, 41(0):665 – 672, 2013.
- Zhang J. and Li V.C. Simulation of crack propagation in fiber-reinforced concrete by fracture mechanics. *Cement and Concrete Research*, 34(2):333 – 339, 2004.